SAPP XXV

25th Symposium on Application of Plasma Processes
and
14th EU-Japan Joint Symposium on Plasma Processing

Book of Contributed Papers

Štrbské Pleso, Slovakia

31 Jan - 5 Feb, 2025

Edited by G. D. Megersa, E. Maťaš, J. Országh, P. Papp, Š. Matejčík

Book of Contributed Papers: 25th Symposium on Application of Plasma Processes and 14th EU-Japan Joint Symposium on Plasma Processing, Štrbské Pleso, Slovakia, 31 January – 5 February 2025.

Symposium organised by Department of Experimental Physics, Faculty of Mathematics, Physics and Informatics, Comenius University in Bratislava and Society for Plasma Research and Applications in hotel SOREA TRIGAN***.

Editors: G. D. Megersa, E. Maťaš, J. Országh, P. Papp, Š. Matejčík

Publisher: Society for Plasma Research and Applications, Bratislava, Slovakia

Issued: January 2025, Bratislava, first issue

ISBN: 978-80-972179-5-2

URL: https://neon.dpp.fmph.uniba.sk/sapp/

Table of Contents

ON MECHANISM OF REACTIVE NITROGEN SPECIES FORMATION IN NEGATIVE POLARITY HIGH PRESSURE GLOW DISCHARGE

Mário Janda[1], Nenad Selaković[2], Olivera Jovanović[2], Neda Babucić[2], Nikola Škoro[2], Oleksandr Galmiz[1], Nevena Puač[2]

[1]*Faculty of mathematics, physics and informatics, Comenius University in Bratislava, Slovakia*
[2]*Institute of Physics, University of Belgrade, Belgrade, Serbia*
E-mail: janda1@uniba.sk

Mass spectroscopy (MS) was used for detection of oxygen and nitrogen species produced by negative polarity high pressure glow discharge (HPGD). Atomic O and N species as well as nitrogen oxides NO and NO_2 were detected. It was not possible to detect ions generated in the discharge directly. As shown by chemical kinetic model, concentration of negative ions is negligible in HPGD because of elevated temperature. Chemical kinetic model was also used to study formation pathways of species detected by MS.

1. Introduction

Electrical discharges can generate chemically active non-equilibrium plasmas, where electrons have significantly higher energy than ions and neutral particles. Among the many types of electrical discharges, low-pressure glow discharges are one of the most common and fundamental, often used for illumination [1]. While less common and well-known than their low-pressure counterparts, high pressure glow discharges (HPGD) offer the possibility of removing organic pollutants from exhaust gases [2]. Furthermore, their stability and efficiency in generating nitric oxide from air make them useful for nitrogen fixation [3].

HPGD can be ignited between a high-voltage metal electrode and a water surface, with the second electrode submerged [4]. This configuration, in combination with the generation of nitrogen oxides in the gas phase, makes HPGD suitable for generating plasma-activated water [5].

Plasma-activated water (PAW) is water that has been exposed to plasma. This exposure infuses the water with reactive oxygen and nitrogen species (RONS), such as hydrogen peroxide, nitrates, and nitrites, which temporarily alter the water's chemical properties and make it useful in many applications in food, agriculture, and biomedicine [6, 7]. These possibilities have made PAW a hot topic in the low-temperature plasma community in recent years.

Despite many studies and obtained results, further research is crucial for a better understanding of the formation mechanisms of reactive species, such as nitrogen oxides, and for assessing the role of different gas-phase species in the formation of aqueous RONS in PAW. From a practical point of view, this knowledge will allow for increased energy efficiency and selectivity with respect to the desired products when generating PAW. For this reason, the formation of RONS by HPGD is studied in this paper, using mass spectrometry (MS) and chemical kinetic modelling. For MS measurements we used molecular beam mass spectrometer (MBMS) that can sample from atmospheric pressure enabling to directly access chemical species created in the plasma. In principle the MBMS can detect both neutral and ionic species but in this study we focused to neutrals.

2. Experimental setup

A schematic diagram of the experimental apparatus is shown in Figure 1. The high pressure glow discharge was generated by a DC high voltage (HV) power supply (Glassmann PSIWH 20R25) with negative polarity output, capable of delivering up to 20 kV. The power supply was connected to the cathode via a 1 MΩ series resistor (R) to limit current. This power supply can also operate as a stabilized current source, providing up to 30 mA.

The cathode consisted of a stainless steel needle with a flat tip and an outer diameter of 0.7 mm. The discharges were generated in dry air from the pressure cylinder (purity 5.0), flowing along the cathode

towards the anode with the gas flow rate of 0.3-0.45 slm, controlled by mass controller (Bronkhorst F201-EV).
For diagnostics of neutral species, a grounded steel ring with an inner diameter of about 4 mm and an outer diameter of about 8 mm served as the anode. This ring was positioned 5 mm in front of the entrance to the mass spectrometer, which had an orifice diameter of 100 µm. For the measurements the mass spectrometer front plate with the orifice was grounded. The cathode-anode gap distance was maintained at 3 mm.
The electrical potential between the cathode and ground was measured using a high voltage probe (Tektronix P6015A) connected to a digital oscilloscope (Keysight MSOX 3024T).
The MBMS used for measurements (Hiden Analytical HPR 60) was operating in two modes- RGA (Residual Gas Analyzer) mode, that provides data on the mass spectra of neutrals in the range 0–100 amu; and MID scan, when the device is set to monitor the temporal changes of selected species. In both cases, for the detection of neutral species a ionization chamber was active with the electron energy set to 70 eV. The MBMS has an internal shutter – Swagelok that allows recording of the background signal coming from the gas phase inside the device.

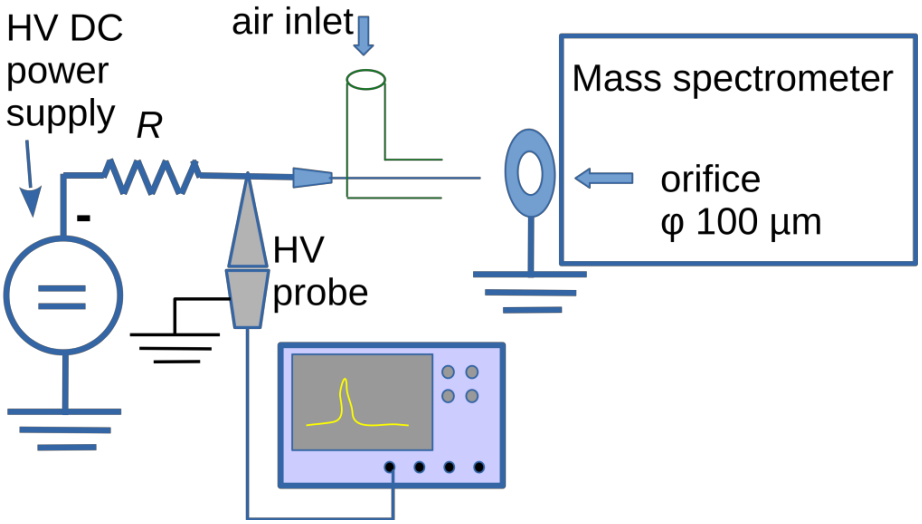

Fig. 1. A schematic diagram of the experimental apparatus.

3. Chemical kinetic model

The aim of the chemical kinetic model is to calculate density evolution of studied species interacting via defined set of chemical reactions. For this purpose we used ZDPlasKin module [8] that includes a Fortran 90 version of the VODE solver for numerical solution of system of ordinary differential equations [9]. Authors of ZDPlasKin also provide a ready-to-use list of plasma chemical processes in nitrogen-oxygen mixtures with all necessary rate coefficients [10]. This set of reactions (version 1.03) includes ~650 chemical reactions among 53 species.
The rate constants of reactions between heavy species from this list are calculated from the thermodynamic gas temperature T_g. The rate constant for electron impact reactions must be calculated from electron energy distribution function (EEDF) obtained by solving the Boltzmann equation for free electrons. The ZDPlasKin package includes a Bolsig+ solver [11] for this purpose. A set of required electron scattering cross sections was taken from the LXCat project database [12].
Finally, ZDPlasKin module requires use of additional subroutines written by user for comprehensive control of simulation conditions, e.g., changes in the gas temperature, pressure and reduced electric field. Our physical model has two parts, glow discharge and afterglow. The afterglow part has to be included because in some experiments, the gas from the discharge did not enter the mass spectrometer directly, but there was a 5 mm gap between the grounded ring electrode and orifice.

For modeling of GD we used constant temperature T_g = 2000 K, constant pressure of 1 atmosphere and constant reduced electric field strength E_n = 60 Td. We also used constant electron density n_e = 10^{12} cm^{-3}. These values were estimated based on previous experimental observations of HPGD [13]. In order to take into account diffusion of species our of the discharge plasma channel and mixing with the surrounding ambient air, we included a primitive diffusion model in our code. After each calculation step with duration Δt, concentration of each heavy particle n_i is decreased by Δn_i calculated as

$$\Delta n_i = -\alpha_{diff}\, n_i\, \Delta t, \qquad (1)$$

where α_{diff} is coefficient representing diffusion of particles out of the plasma channel. To keep constant pressure (total density of particles), the removed particles were replaced by N_2 and O_2 molecules (ratio 4:1). This simulates mixing with the ambient air.

In the second part of the model, an afterglow period of 0.2 s, the reduced electric field strength decreased exponentially to 3 Td with a time constant of 20 ns. Electrons concentration was calculated dynamically along with the densities of all other species, rather than being held constant. Mixing with the surrounding air continued during the afterglow phase, leading to a calculated decrease in gas temperature. Electron diffusion was also incorporated, with a diffusion coefficient ten times higher than that of the heavy particles.

4. Results and Discussion

HPGD was generated with discharge current of either 2.1 mA, or 3 mA. The applied voltage was -3 kV and -4 kV, respectively. The discharge voltage (across the gap) decreased from ~1.3 kV to ~1.15 kV when the HPGD current increased from 2.1 mA to 3 mA. Mass spectra of produced neutral species were measured for both discharge currents. The obtained spectra had the same species visible for both currents so in Figure 2 we present the data recorded for 3 mA.

The data shows only species created in the plasma as the background signal, recorded in plasma off conditions, was subtracted. The most abundant species created in the discharge were atoms of H,N and O and reactive species OH, H_3O, NO, H_2O_2 and N_2O.

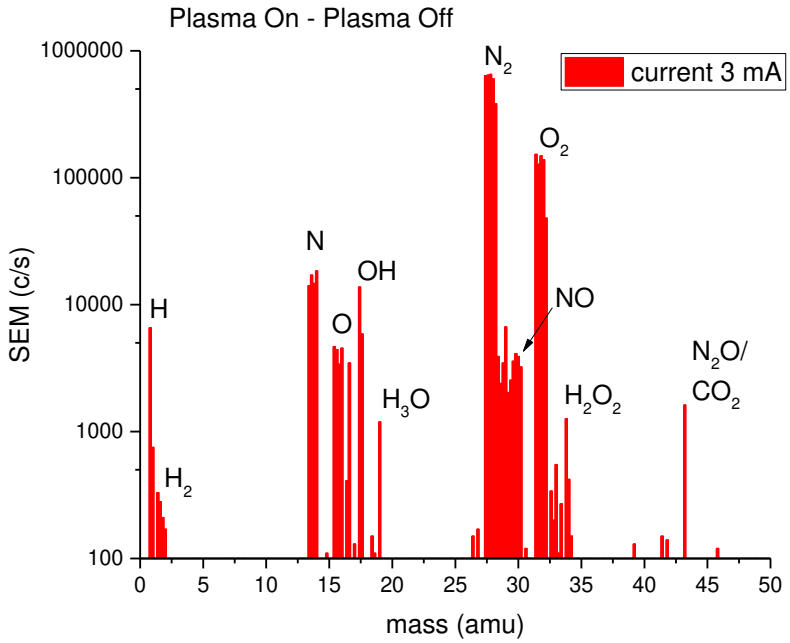

Fig. 2. Mass spectra of neutral species measured for current 3 mA.

In the MID scan mode, we monitored temporal changes in the nitrogen species NO, N_2O and NO_2 important for PAW generation. In Figure 3 we show recorded signals for these species with respect to different measurements conditions. Measurements were conducted with Swagelok open and with Swagelok closed. Swagelok open represents the sum of foreground and background species, while Swagelok closed corresponds to background species only. For the first 6 minutes of recording the discharge was off so variations in the signal is only due to processes inside the device. Once the discharge is ignited, increase in NO and NO_2 signals was due to the species created in the discharge. Obviously, creation of N_2O species was not large so the signal did not change after discharge inception.

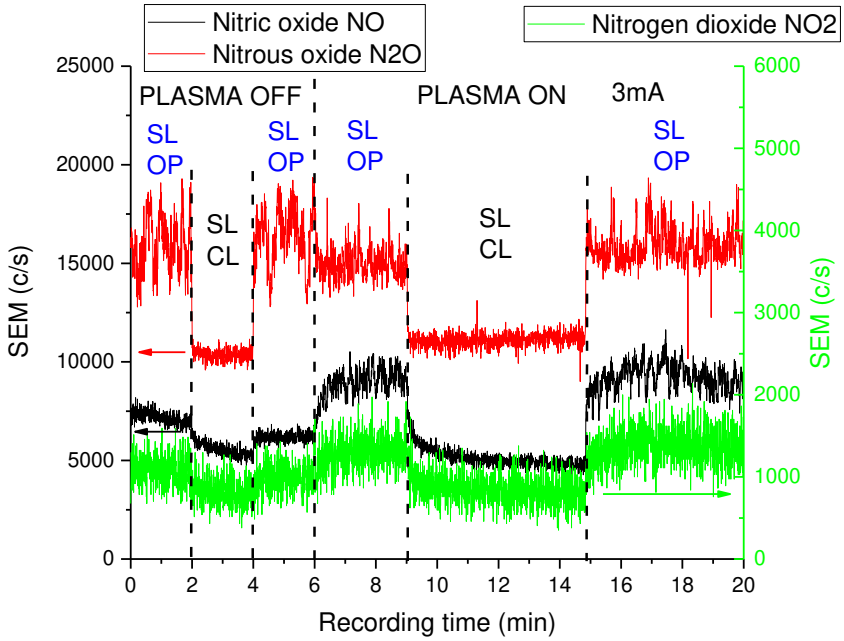

Fig. 3. MID-scan of NO, NO_2 and N_2O species without and with the discharge operating in front of the MS orifice with addition of synthetic air. Discharge current was 3 mA. Measurements were perforemed with Swagelok closed (SL CL) and open (SW OP).

In summary, the experimental data confirmed generation of N, O, NO and NO_2 by HPGD. Chemical kinetic model using ZDPlasKin module was used to explain their formation. As for example, Figure 4 shows time evolution of N, O, NO, NO_2 and O_3 species concentrations in the glow discharge. This calculation was performed with $\alpha_{diff} = 2\ s^{-1}$.

Our model incorporates diffusion, but the employed calculation approach is simplified, and the exact value of the diffusion coefficient remains unknown. Instead, we utilize a parameter, α_{diff}, to represent the diffusion rate. We performed several calculations with α_{diff} ranging from 0.1 to 10 s^{-1}. Since α_{diff} influences the calculated steady-state concentrations of species in the plasma, we cannot definitively determine the actual concentrations of the studied species in the HPGD. However, we observed that α_{diff} in studied range does not significantly affect the ratio of concentrations of various RONS or their production pathways.

Figure 4 demonstrates that the concentrations of all studied RONS reach a steady state after approximately 0.2 ms, remaining constant thereafter. This steady state arises from a balance between production (through chemical reactions) and removal (via chemical reactions and diffusion). Consequently, we analyzed the reaction pathways separately for the initial phase of the simulation and for the subsequent steady state.

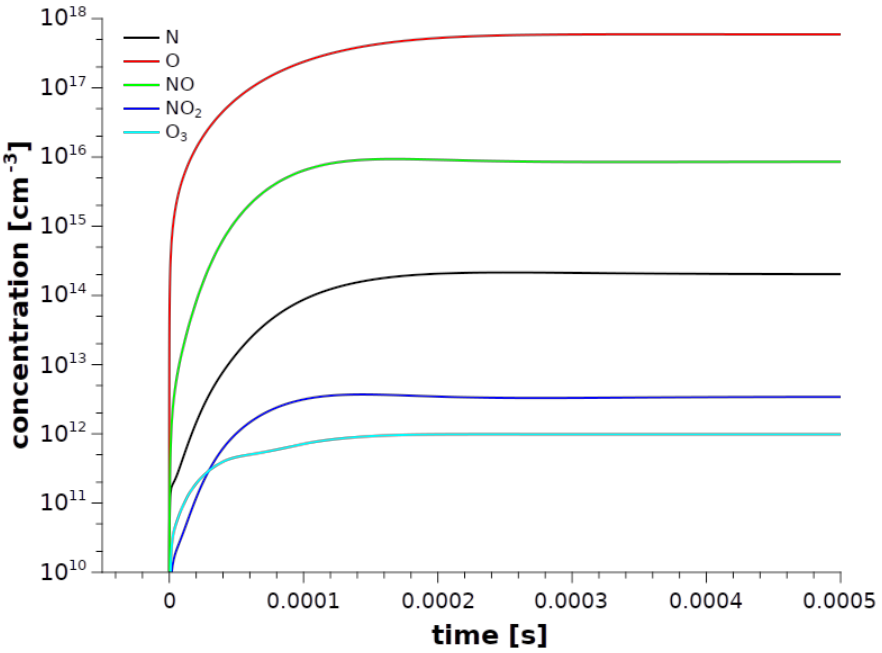

Fig. 4. Time evolution of N, O, NO, NO_2 and O_3 species concentration; calculated with $\alpha_{diff} = 2\ s^{-1}$.

In the initial phase (Figure 5), O atoms are mainly produced by reactions of O_2 with electronically excited molecular nitrogen species N_2* (the most important being $N_2(B^3\Sigma)$, and by electron impact dissociation of O_2 molecules:

$N_2^* + O_2 \rightarrow N_2 + O + O,$ (2)
$e + O_2 \rightarrow e + O + O.$ (3)

Contribution of other reactions, such as

$N + O_2 \rightarrow O + NO$ (4)

on O atoms production is already quite small.
In the later steady state phase, the production reactions (2-4) are compensated by O atoms recombination reactions

$O + O + M\ (M = O, O_2, N_2) \rightarrow O_2 + M.$ (5)

In this simplified O production/removal mechanism we omitted reactions between O, $O(^1D)$ and $O(^1S)$ species. An equilibrium between these species is achieved quickly, with O representing more than 99.9% of them.
N atoms are produced mostly by these two reactions:

$O(^1D) + NO \rightarrow O_2 + N,$ (6)
$N_2(a^{`1}) + NO \rightarrow N_2 + N + O.$ (7)

There is also a third important reaction producing N atoms, electron impact dissociacion of N_2, but it plays an important role at the very beginning of the simulation ($t < 50\ \mu s$), when there is still not enough NO molecules for N generation by equations (6) and (7).

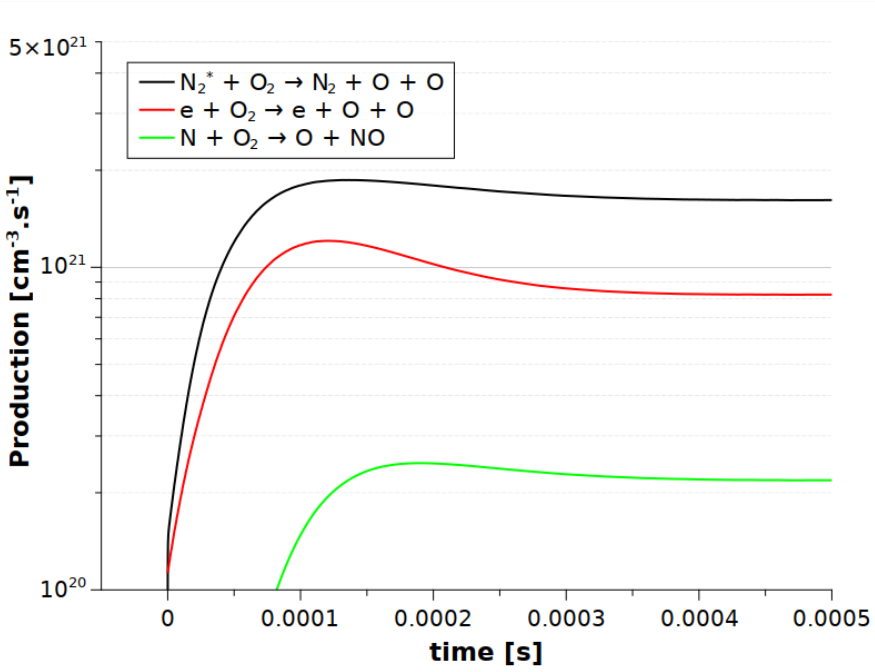

Fig. 5. Production of O atoms during the initial phase of the simulation; calculated with $\alpha_{diff} = 2\ s^{-1}$.

In steady state, the removal of NO molecules by N (equations (6) and (7)) is compensated by NO production via reaction

$N + O_2 \rightarrow O + NO.$ (8)

Reactions (6-8) all involve NO, they are crucial not only for N production and losses, but they also influence the density of NO. Reaction (8) is actually the most important for NO production (Figure 6). The other two important reactions are

$N_2(A^3) + O \rightarrow NO + N(^2D),$ (9)
$N(^2D) + O_2 \rightarrow NO + N.$ (10)

In the steady state, the production of NO is compensated by its removal (Figure 7) via reactions (6), (7), (11) and (12)

$NO + N(^2D) \rightarrow N_2 + O,$ (11)
$NO + N \rightarrow N_2 + O.$ (12)

NO_2 is produced almost eclusively by reaction (13) and removed by reaction (14)

$O + NO + M \rightarrow NO_2 + M\ (N_2, O_2),$ (13)
$O + NO_2 \rightarrow NO + O_2.$ (14)

Steady state NO_2 concentration $[NO_2]$ can be therefore easily calculated as $[NO_2] = k_{13}.[NO]/k_{14}$, assuming balance between NO_2 production and destruction by reactions (13) and (14). In this formula, [NO] is steady state concentration of NO, k_{13} and k_{14} are rate coefficients of reactions (13) and (14), respectively. At 2000 K, the ratio of these two rate coefficients is 7.3×10^{-4} and it explains why the steady state concentration of NO_2 is much lower than the concentration of NO (Figure 4).

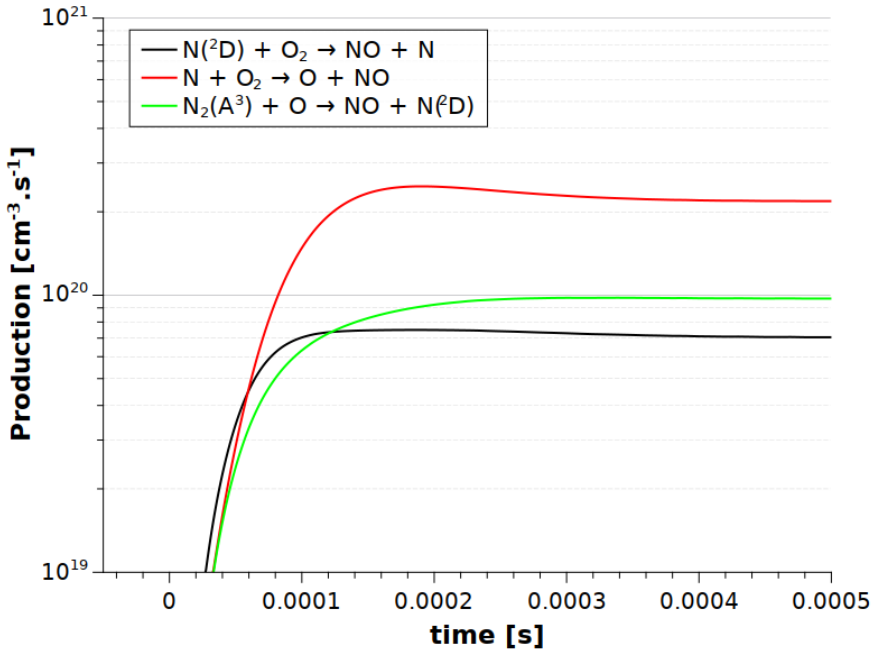

Fig. 6. Main reactions responsible for production of NO molecules; calculated with α_{diff} = 2 s^{-1}.

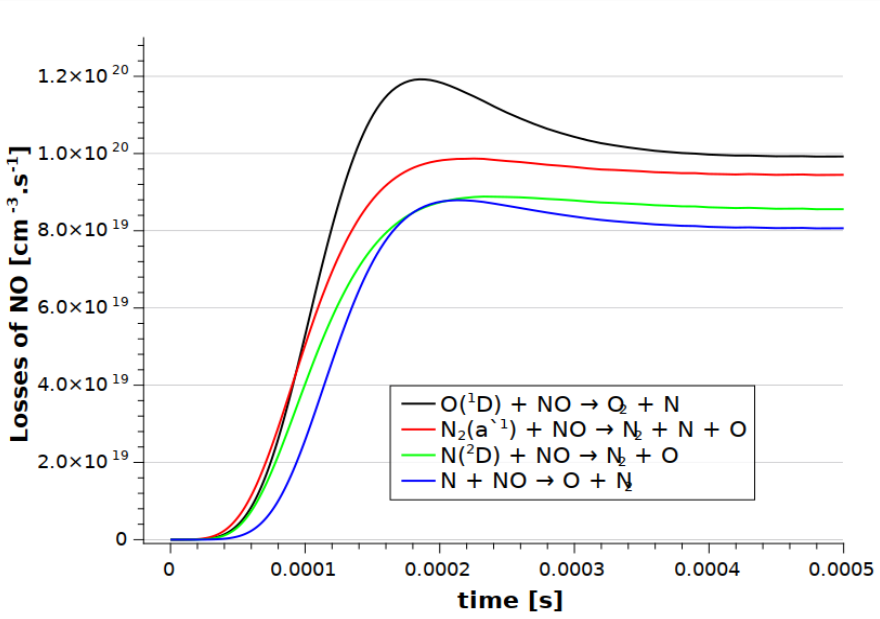

Fig. 7. Main reactions responsible for losses of NO molecules; calculated with α_{diff} = 2 s^{-1}.

Based o *ex-situ* measurements of the gas after treatment by glow discharge, the concentration of NO is higher than the concentration of NO_2, but the difference is not so significant [3]. Final NO and NO_2 concentration is mainly determined by reactions in the gas after leaving the discharge zone (afterglow). Figure 8 shows time evolution of gas temperature and N, O, NO and NO_2 species concentrations in the discharge afterglow, calculated with α_{diff} = 10 s^{-1}. The concentration of atomic species (N and O) decreases rapidly. While the NO concentration decreases slowly, the NO_2 concentration increases, despite mixing with the ambient air. Consequently, the difference between NO and NO_2 concentrations decreases in the discharge afterglow.

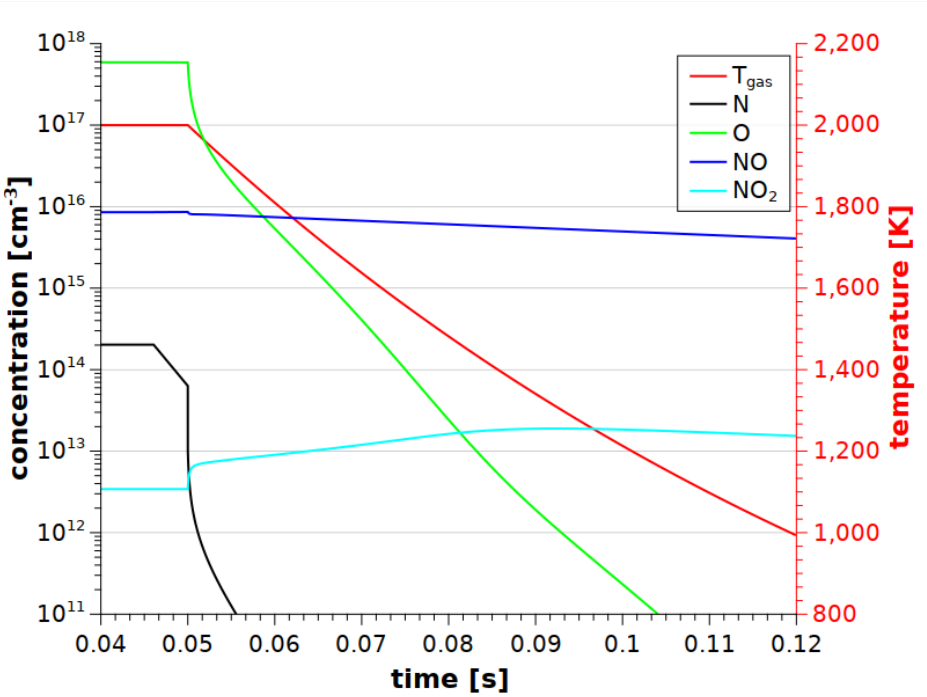

Fig. 8. Time evolution the gas temperature and N, O, NO and NO_2 species concentrations; calculated with α_{diff} = 10 s^{-1}.

A stable signal from ions directly generated by the HPGD was not detected by mass spectrometry. This can be attributed to two main factors. Firstly, the HPGD migrated on the surface of the orifice plate that served as anode, making its position relative to the spectrometer's gas entrance (a 100 µm orifice) highly variable. A stable ion signal could only be observed if the HPGD was positioned directly above this orifice, which occurred only randomly and occasionally. Secondly, even with the discharge positioned stably above the orifice, ion detection remains challenging. Positive ions are repelled from the anode, and the concentration of negative ions within the HPGD is relatively low, according to the kinetic model. The dominant negative ion, O^-, has a concentration of approximately 10^{10} cm^{-3}, two orders of magnitude lower than the electron concentration. This low negative ion concentration may be due to the elevated gas temperature in the HPGD plasma channel.

5. Conclusions

Fixation of nitrogen from the air, converting it into reactive compounds, remains a significant challenge and a hot topic within the low-temperature plasma community. High-pressure glow discharges offer a stable and efficient means to generate nitrogen oxides, key precursors for nitrogen fixation. This study investigates the mechanisms of nitrogen oxide generation in an HPGD using a combined approach of mass spectrometry and chemical kinetic modeling.

Mass spectrometry provided insights into the types of reactive oxygen and nitrogen species produced, while the kinetic model simulated the complex chemical reactions within the plasma. Our findings shed light on the dominant reaction pathways on nitrogen oxide formation. However, further research is crucial to refine our understanding. Future experimental work should focus on improving the detection and quantification of reactive species, particularly ions. Model enhancements are also necessary, including a more accurate representation of diffusion processes and the discharge afterglow phase. Furthermore, incorporating additional chemical reactions involving water molecules will enable us to explore the crucial role of humidity in the generation of nitrogen oxides, nitric acid, and nitrous acid. This comprehensive approach promises to advance our knowledge of nitrogen fixation using HPGD

and pave the way for the development of efficient and sustainable plasma-based technologies for fertilizer production and other applications.

Acknowledgement: Supported by the project of bilateral cooperation between Republic of Serbia and Republic of Slovakia 2024-2025 (project no. 337-00-3/2024-05/07 and APVV SK-SRB-23-0043); grant of the Ministry of Science, Technological Development and Innovations no. 451-03-68/2024-14/200024; and VEGA project No. 1/0596/22.

6. References

[1] Claude G 1913 *The Engineering Magazine* **115** 271–274.
[2] Machala Z, Laux C O and Kruger C H 2005 *IEEE Trans. Plasma Sci. - Special Issue on Plasma Images* **33** 320-321.
[3] Janda M, Hensel K, Machala Z and Field T A 2023 *J. Phys. D Appl. Phys.* **56** 485202
[4] Janda M, Machala Z, Morvová M, and Morva I 2008 *Orig. Life Evol. Biosph.* **38** 23-35
[5] Pai D Z 2021 *Journal of Physics D: Applied Physics* **54** 355201
[6] Rathore V, Tiwari B S and Nema S K 2021 Plasma Chem Plasma Process. **42** 109-129
[7] Chen Z, Xu R-G, Chen P and Wang Q 2020 *IEEE Trans. Plasma Sci.* **48** 3455–3471.
[8] Pancheshnyi S et al. 2008 Computer Code ZDPlasKin, Univ. Toulouse, Toulouse, LAPLACE, CNRS-UPS-INP, France. [Online]. Available: https://www.zdplaskin.laplace.univ-tlse.fr
[9] Brown P N, Byrne G D and Hindmarsh A C 1989 *SIAM J. Sci. Stat. Comput.* **10** 1038–1051
[10] kinet_N2_O2_v1.03 2015 [Online]. Available: http://www.zdplaskin.laplace.univ-tlse.fr/wp-content/uploads/2015/08/kinet_N2_O2_v1.03.inp
[11] Hagelaar G J M and Pitchford L C 2005 Plasma Sources Sci. Technol. **14** 722-733
[12] Pancheshnyi S et al. 2012 *Chem. Phys.* **398** 148–153.
[13] Machala Z et al. 2007 *J. Molec. Spectrosc.* **243** 194-201.